Dalton Transactions

Cite this: *Dalton Trans.*, 2011, **40**, 3455

www.rsc.org/dalton

COMMUNICATION

Formation and characterization of a six-coordinate iron(III) complex with the most ruffled porphyrin ring†

Akira Ikezaki[a,b] **and Mikio Nakamura***[a,b,c]

Received 30th December 2010, Accepted 8th February 2011
DOI: 10.1039/c1dt10042d

The six-coordinate iron(III) porphyrin complex, [Fe(T^{i}PrP)(2-MeBzIm)$_2$]$^+$, having the most ruffled porphyrin ring shows some unusual properties; the complex adopts the pure (d_{xz}, d_{yz})^4(d_{xy})^1 ground state below 200 K in spite of the coordination of an imidazole ligand and exhibits the rare spin transition to the (d_{xz}, d_{yz})^3(d_{xy})^1(d_{z2})^1 state at higher temperature.

The ruffled metal porphyrinates exhibit a wide variety of properties that are different from those of the corresponding planar porphyrinates.[1–4] One of the most striking features should be the bathochromic shift in the UV-Vis spectra.[5] Thus, Zn(T^{t}BuP)(py), which has the most ruffled porphyrin ring among zinc porphyrinates, shows the Soret band at 462 nm as compared with 432 nm in less ruffled Zn(T^{n}BuP)(py).[6,7] If the metal ions are paramagnetic, the magnetic properties should also be perturbed by the ring deformation.[8] We have been studying how the physicochemical properties of iron(III) porphyrinates are affected by the deformation of the porphyrin ring.[1,2] To understand the effects of ring deformation on the electronic and magnetic behaviors, we need a highly ruffled complex caused mainly by the steric effect; some low-spin iron(III) porphyrinates can be deformed solely by electronic reasons.[9–11] Such a complex can be obtained by the combination of ruffled Fe(TRP)ClO_4 and a sterically very hindered substituted imidazole ligand(RIm).[12–16] In this paper, we will describe that [Fe(T^{i}PrP)(2-MeBzIm)$_2$]ClO_4 (**1**) is the most ruffled low-spin iron(III) porphyrinate and that **1** exhibits quite unusual magnetic behaviors which are different from those of less ruffled bis(imidazole) complexes.

The crystals of **1** were obtained by the addition of cyclohexane to the $CHCl_3$ solution containing Fe(T^{i}PrP)ClO_4 and 6 equiv of 2-MeBzIm. Fig. 1 shows the crystal structure of **1** determined by the X-ray crystallographic analysis. As is clear from Fig. 1(a), the porphyrin ring is extremely ruffled. The average ruffling dihedral angle between two diagonal pyrrole rings reaches as much as 57.3°,

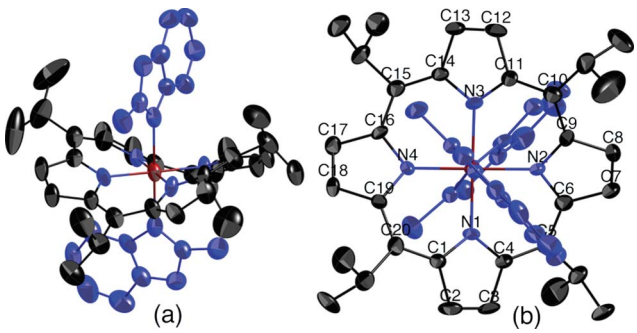

Fig. 1 Molecular structure of **1**; (a) side view and (b) top view. Thermal ellipsoids are drawn to enclose 50% probability.

which is much larger than that of [Zn(T^{t}BuP)(py)]; *i.e.*, 52.6°.[7] The projections of the two 2-MeBzIm planes against the porphyrin core almost exactly bisect adjacent pairs of N_P–Fe–N_P angles as shown in Fig. 1(b), *i.e.* 44.6° and 44.0°. Thus, the dihedral angle between the two imidazole ligands is 89.4°. The deviation of the peripheral carbon atoms from the mean plane of the 24-atom core is shown in Fig. 2. The average deviation of the *meso* carbon atoms is 0.92 Å, which is comparable in magnitude to that of [Zn(T^{t}BuP)(py)], *i.e.* 0.90 Å.[7]

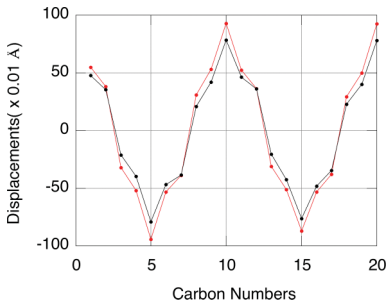

Fig. 2 Displacements of the peripheral carbon atoms of **1**(red) and **2**(black) from the mean plane of the 24-atom core.

Because of the strongly ruffled structure, the average Fe–N_P distance is extremely short, *i.e.* 1.915(5) Å. To our knowledge, this is the shortest distance in iron porphyrinates reported previously. Corresponding to the extremely short Fe–N_P lengths, the average Fe–N_{axial} length is fairly long, 2.070(5) Å, which should be ascribed to the steric repulsion between 2-MeBzIm and porphyrin core as shown in Fig. S1 of the Supporting Information.† The structural

[a]*Department of Chemistry, School of Medicine, Toho University, Ota-ku, Tokyo, 143-8540, Japan. E-mail: mnakamu@med.toho-u.ac.jp*
[b]*Research Center of Materials with Integrated Properties, Toho University, Funabashi, 274-8510, Japan*
[c]*Division of Chemistry, Graduate School of Science, Toho University, Funabashi, 274-8510, Japan*

† Electronic supplementary information (ESI) available. CCDC reference numbers 807917 and 807918. For ESI and crystallographic data in CIF or other electronic format see DOI: 10.1039/c1dt10042d

Table 1 Structural and spectroscopic parameters of ruffled low-spin $[Fe^{III}(Por)L_2]^+$

Complexes	Por	L	Fe–N_p	Fe–L	ΔC_{meso} [a]	ω[b]	ref
1	T^iPrP	2-MeBzIm	1.915(5)	2.070(5)	0.92	57.3	This work
2	T^iPrP	HIm	1.938(3)	1.993(3)	0.78	47.9	This work
3	TMP	1,2-Me_2Im	1.937(12)	2.004(5)	0.72	45.0	12
4	TEtP	2-MeIm	1.932(14)	2.017(12)	0.71	46.5	13
5	TPP	4-CNPy	1.952(7)	2.002(8)	0.55	36.3	10
6	TMP	DMAP	1.964(10)	1.984(8)	0.51	32.1	9
7	TMP	3-EtPy	1.961(4)	2.000(9)	0.43	[c]	10
8	TMP	4-CNPy	1.961(7)	2.011(14)	0.41	26.6	14
9	TPP	2-MeIm	1.970(4)	2.012(8)	0.39	26.3	15
10	TMP	3-ClPy	1.968(2)	2.012(8)	0.36	[c]	10

[a] Deviation of the *meso* carbon atoms from the mean plane of the 24-atom core. [b] Dihedral angle between diagonal pyrrole rings. [c] Data are not available.

parameters of **1** are summarized in Table 1.[9,10,12–15] Crystal data and structural refinement for **1** and **2** are listed in Tables S-1 and S-2,† respectively.

To reveal the effect of bulky imidazole ligand on the porphyrin structure, the molecular structure of $[Fe(T^iPrP)(HIm)_2]ClO_4$(**2**) has also be determined as shown in Fig. S2. †The average ruffling dihedral angle is 47.9° which is by 9.5° smaller than that of **1**. Correspondingly, the average Fe–N_P length has increased to 1.938(3) Å while the average Fe–N_{axial} length has decreased to 1.993(3) Å. Fig. 2 shows the deviation of the peripheral carbon atoms, which clearly indicates that the ruffling of the porphyrin ring decreases as the axial ligand changes from 2-MeBzIm to HIm. The structural parameters of **2** are also listed in Table 1 together with those of analogous low-spin iron(III) complexes (**3**–**10**) carrying nitrogen bases such as imidazoles and pyridines at the axial positions.[9,10,12–15] Fig. 3 shows the correlation between the Fe–N_p bond lengths and the out-of-plane displacements of the *meso* carbon atoms. The data in Table 1 together with the correlation diagram shown in Fig. 3 clearly indicate that **1** has the most ruffled porphyrin ring as is revealed from the shortest Fe–N_p bond length, the largest ruffling dihedral angle, and the largest out-of-plane displacement of the *meso* carbon atoms.

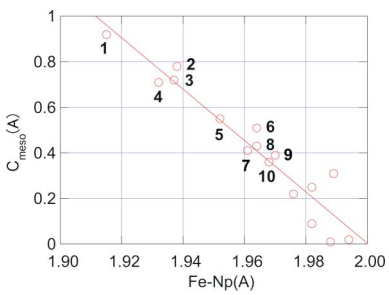

Fig. 3 Correlation between Fe–Np bondlength and the out-of-plane deviation of the *meso* carbons. Numbers in the graph correspond to the complexes shown in Table 1.

Having found that **1** has the most ruffled porphyrin ring among the low-spin ferric porphyrinates reported previously, we have then examined if the complex exhibits some unique properties that have never been observed in less deformed complexes. The nonplanarity of the porphyrin ring is sensitively reflected by the UV-Vis spectroscopy because the deformed ring destabilizes the HOMO while it tends to maintain the energy level of LUMO. In fact, the UV-Vis spectrum of **1** has shown the absorption maxima at 432, 532, 578, and 620 nm in CH_2Cl_2 solution while those of **2** are 422, 536, 574, and 614 nm.

The ^1H NMR spectrum of **1** taken at 298 K in CD_2Cl_2 solution is given in Fig. S3.† The *meso*-CH and pyrrole-H signals appear at 21.2 and 3.47 ppm, respectively, which should be compared with the corresponding signals, 5.08 and −12.2 ppm, of $[Fe(T^nPrP)(HIm)_2]^+$ adopting the S = 1/2(d_π) ground state.[17] Hereafter, the $(d_{xy})^2(d_{xz}, d_{yz})^3$, $(d_{xz}, d_{yz})^4(d_{xy})^1$, and $(d_{xz}, d_{yz})^3(d_{xy})^1(d_{z2})^1$ ground states are abbreviated as S = 1/2(d_π), S = 1/2(d_{xy}), and S = 3/2(d_{xy}), respectively. Fig. 4(a) shows the Curie plots of the *meso*-CH signals of **1** and **2** where the symbols and lines are given in red and black, respectively.[17] The large downfield shift of the *meso*-CH signals in **1** and **2** is a direct indication that the *meso* carbon atoms have sizable amount of spin densities, which in turn indicates that these two complexes adopt the S = 1/2(d_{xy}) ground state. As shown in Fig. 4(a), the Curie plots of the *meso*-CH signal of **1** has exhibited a slight curvature above 223 K ($1/T < 0.00448$ K^{-1}). Similar tendency has been observed in the Curie plots of the pyrrole-H signals given in Fig. 4(b). The deviation is much larger in the pyrrole-H than in the *meso*-CH signal. The result strongly indicates that the spin state of **1** is changing from the S = 1/2(d_{xy}) to the S = 3/2(d_{xy}) ground state as the temperature is raised.[8,18,19] For comparison, the Curie plots of the pyrrole-H signal of the bis(benzaldehyde) complex $[Fe(T^iPrP)(PhCHO)_2]^+$ adopting the S = 3/2(d_{xy}) is also given in Fig. 4(b).[20–22] If we assume that **1** exists as an equilibrium mixture of the two spin isomers with the S = 1/2(d_{xy}) and S = 3/2(d_{xy}) at 298 K as shown

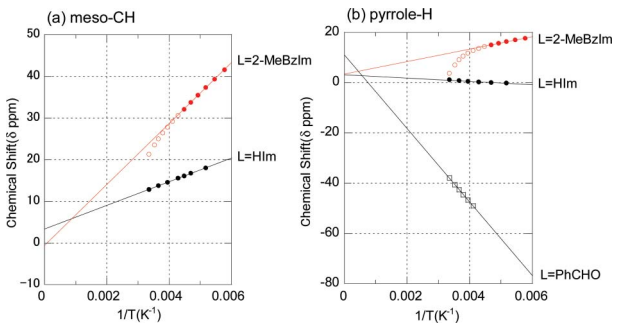

Fig. 4 Curie plots of (a) *meso*-CH and (b) pyrrole-H signals of **1** and **2**, where red open circle and red filled circle indicate the chemical shifts of **1** at higher and lower temperature, respectively. The black open square indicates the chemical shift of $[Fe(T^iPrP)(PhCHO)_2]^+$ that adopts the S = 3/2(d_{xy}) ground state.

in (1), the population of the S = 1/2(d_{xy}) is estimated to be *ca.* 85%.

$$S = 1/2(d_{xy}) \rightleftarrows S = 3/2(d_{xy}) \quad (1)$$

Fig. 5 shows the EPR spectrum of **1** taken in frozen CH_2Cl_2 solution at 4.2 K. The computer simulation of the observed spectrum has yielded the $g_\perp$ and g_{II} values to be 2.542 and 1.474, respectively, which is consistent with the NMR result that the complex adopts the S = 1/2(d_{xy}) ground state at lower temperature. The tetragonality parameter (Δ) has been determined to be –2.67 λ, which indicates that the d_{xy} orbital is located above the d_π orbitals by 2.76λ, where λ is a spin orbit coupling constant.[3] Curiously, the EPR spectrum of **2** is quite similar to that of **1** as far as the g values are concerned; the $g_\perp$ = 2.55 and g_{II} = n.d. in the case of **2**.[17] Thus, the energy gap between the d_{xy} and d_π orbitals of **2** could be similar to that of **1** at 4.2 K. It should be noted, however, that the line width of the $g_\perp$ signal of **2** is nearly six times as much as that of **1**.

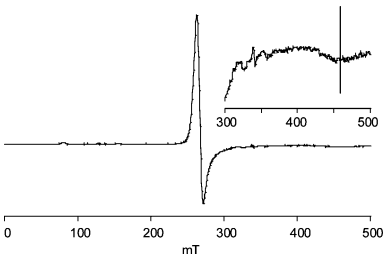

Fig. 5 EPR spectra of **1** taken in frozen CH_2Cl_2 solution at 4.2 K with microwave frequency 9.493 GHz.

As mentioned above, the Curie plots of the pyrrole-H and *meso*-CH signals have suggested the presence of a quite rare spin transition from the S = 1/2(d_{xy}) to the S = 3/2(d_{xy}) as the temperature is raised. In order to further reveal the magnetic behavior of **1**, we have measured the effective magnetic moments (μ_{eff}) in CD_2Cl_2 solution by the Evans method. As shown in Fig. 6, the μ_{eff} value is constant, 2.1 B.M., in the temperature range 173 to 203 K. As the temperature is further raised, the magnetic moment gradually increases and reaches 2.9 B.M. at 298 K. Since the spin-only value expected for the S = 3/2 complex is 3.87 B.M., the population of the spin isomer with the S = 1/2(d_{xy}) is estimated to be 61%.[23] The value is much smaller than the one determined by the NMR data, which should be ascribed to the underestimation of the effective magnetic moment of the pure intermediate-spin complex.

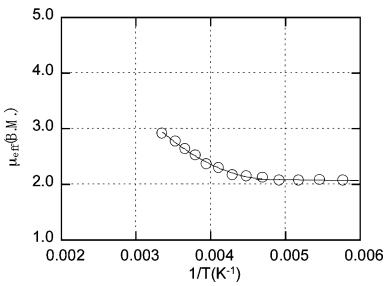

Fig. 6 Temperature dependence of the effective magnetic moments of **1** determined by the Evans method.

Fig. 7 shows the ^{13}C NMR spectra of **1** taken in CD_2Cl_2 solution at 298 K. The most characteristic feature is the large downfield shift of the *meso* carbon signal, *i.e.* 466 ppm, as compared with 356(ave), 287, and 84.9 ppm for $[Fe(T^iPrP)(2\text{-}MeIm)_2]^+$, $[Fe(T^iPrP)(HIm)_2]^+$, and $[Fe(T^nPrP)(HIm)_2]^+$, respectively.[17,24] It should be noted that all the complexes carrying imidazole or substituted imidazole adopt the S = 1/2(d_π) ground state and exhibits the *meso* carbon signal slightly more upfield than their diamagnetic positions as typified by $[Fe(T^nPrP)(HIm)_2]^+$. A very few exceptional cases are $[Fe(T^iPrP)(2\text{-}MeIm)_2]^+$ and $[Fe(T^iPrP)(HIm)_2]^+$; they exist mainly as the isomer with the S = 1/2(d_{xy}) ground state in the equilibrium given by eqn (2).

$$S = 1/2(d_{xy}) \rightleftarrows S = 1/2(d_x) \quad (2)$$

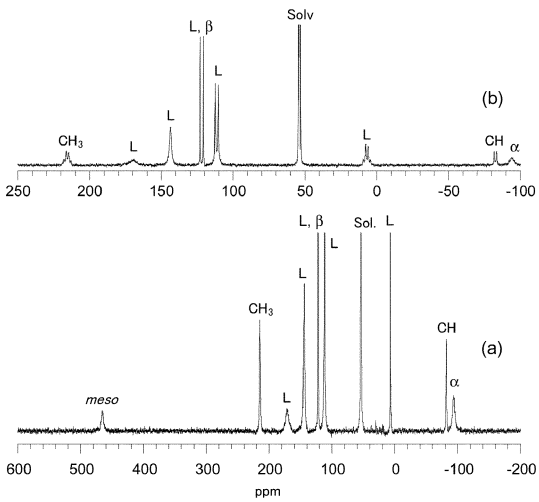

Fig. 7 ^{13}C NMR spectra of **1** taken in CD_2Cl_2 solution at 298 K: (a) ^1H decoupled and (b) ^1H coupled spectra. Signals labeled as *meso*, α, β, CH, CH_3, L, and Solv are ascribed to the *meso*, pyrrole-α, pyrrole-β, *meso*-CH, *meso*-CH_3, ligand, and solvent carbon atoms, respectively.

The fact that **1** exhibits the *meso* signal most downfield among all the iron(III) porphyrinates carrying imidazole or its derivatives suggests that the enegy gap between the d_{xy} and d_π orbitals is the largest in **1**. In other words, the d_{xy} orbital is greatly destabilized by the strong interaction with the a_{2u}-like orbital caused by the most ruffled porphyrin structure. In addition, the long Fe–N_{axial} bond length caused by the severe steric repulsion between the 2-MeBzIm ligand and ruffled porphyrin core stabilizes the d_{z^2} orbital. Consequently, the spin transition occurs from the S = 1/2(d_{xy}) to the S = 3/2(d_{xy}) state as the temperature is raised.

In conclusion, we have shown that **1** has the most ruffled porphyrin ring among all the iron porphyrinates. Because of the extremely ruffled structure, the complex adopts the pure S = 1/2(d_{xy}) ground state below 200 K in spite of the coordination of imidazole ligands and exhibits a quite unusual spin transition from the S = 1/2(d_{xy}) to the S = 3/2(d_{xy}) as the temperature is raised.

This work was supported by the Grant-in-Aid for Scientific Research (No. 21750175 and No 22550157) from Ministry of Education, Culture, Sports, Science and Technology, Japan. This work was also supported by the Research Center for Materials with Integrated Properties, Toho University, and the Project Research

Grant (No. 20-4 to A.I.) of School of Medicine, Toho University. Thanks are due to the Research Center for Molecular-Scale Nanoscience, the Institute for Molecular Science (IMS).

Notes and references

1 M. Nakamura, Y. Ohgo and A. Ikezaki, Electronic and Magnetic Structures of Iron Porphyrin Complexes, In *Handbook of Porphyrin Science*, K. M Kadish, K. M Smith and R. Guilard, ed., World Scientific, 2010, pp 1–146.

2 M. Nakamura, *Coord. Chem. Rev.*, 2006, **250**, 2271–2294.

3 J. A. Shelnutt, X.-Z. Song, J.-G. Ma, S.-L. Jia, W. Jentzen and C. J. Medforth, *Chem. Soc. Rev.*, 1998, **27**, 31–41.

4 R. Patra, S. Bhowmik, S. K. Ghosh and S. P. Rath, *Dalton Trans.*, 2010, **39**, 5795–5806.

5 J. S. Evans and R. L. Musselman, *Inorg. Chem.*, 2004, **43**, 5613–5629.

6 Abbreviations. 2-MeBzIm: 2-Methylbenzimidazole. HIm: imidazole. T^{t}BuP, T^{n}BuP, T^{i}PrP, T^{n}PrP, and TRP: Dianions of 5,10,15,20-tetra(*tert*-butyl)porphyrin, 5,10,15,20-tetra(*n*-butyl)porphyrin, 5,10,15,20-tetra(isopropyl)porphyrin, 5,10,15,20-tetra(propyl)porphyrin, and 5,10,15,20-tetra(alkyl)porphyrin, respectively.

7 T. Ema, M. O. Senge, N. Y. Nelson, H. Ogoshi and K. M. Smith, *Angew. Chem., Int. Ed. Engl.*, 1994, **33**, 1879–1881.

8 T. Ikeue, Y. Ohgo, T. Yamaguchi, M. Takahashi, M. Takeda and M. Nakamura, *Angew. Chem., Int. Ed.*, 2001, **40**, 2617–2620.

9 M. K. Safo, G. P. Gupta, F. A. Walker and W. R. Scheidt, *J. Am. Chem. Soc.*, 1991, **113**, 5497–5510.

10 M. K. Safo, F. A. Walker, A. M. Raitsimring, W. P. Walters, D. P. Dolata, P. G. Debrunner and W. R. Scheidt, *J. Am. Chem. Soc.*, 1994, **116**, 7760–7770.

11 G. Simonneaux, V. Schünemann, C. Morice, L. Carel, L. Toupet, H. Winkler, A. X. Trautwein and F. A. Walker, *J. Am. Chem. Soc.*, 2000, **122**, 4366–4377.

12 O. Q. Munro, H. M. Marques, P. G. Debrunner, K. Mohanrao and W. R. Scheidt, *J. Am. Chem. Soc.*, 1995, **117**, 935–954.

13 Y. Ohgo, T. Ikeue, T. Saitoh and M. Nakamura, *Chem. Lett.*, 2002, **31**, 432–433.

14 M. K. Safo, G. P. Gupta, C. T. Watson, U. Simonis, F. A. Walker and W. R. Scheidt, *J. Am. Chem. Soc.*, 1992, **114**, 7066–7075.

15 W. R. Scheidt;, J. F. Kirner;, J. L. Hoard and C. A. Reed, *J. Am. Chem. Soc.*, 1987, **109**, 1963–1968.

16 M. Nakamura and N. Nakamura, *Chem. Lett.*, 1991, **20**, 1885–1888.

17 T. Ikeue, Y. Ohgo, T. Saitoh, M. Nakamura, H. Fujii and M. Yokoyama, *J. Am. Chem. Soc.*, 2000, **122**, 4068–4076.

18 T. Ikeue, Y. Ohgo, O. Ongayi, M. G. H. Vicente and M. Nakamura, *Inorg. Chem.*, 2003, **42**, 5560–5571.

19 A. Ikezaki, M. Takahashi and M. Nakamura, *Angew. Chem., Int. Ed.*, 2009, **48**, 6300–6303.

20 A. Ikezaki, Y. Ohgo, T. Watanabe and M. Nakamura, *Inorg. Chem. Commun.*, 2008, **11**, 1198–1201.

21 R.-J. Cheng, Y.-K. Wang, P.-Y. Chen, Y.-P. Han and C.-C. Chang, *Chem. Commun.*, 2005, 1312–1314.

22 Y. Ling and Y. Zhang, *J. Am. Chem. Soc.*, 2009, **131**, 6386–6388.

23 Y.-P. Huang and R. J. Kassner, *J. Am. Chem. Soc.*, 1979, **101**, 5807–5810.

24 T. Ikeue, Y. Ohgo, T. Saitoh, T. Yamaguchi and M. Nakamura, *Inorg. Chem.*, 2001, **40**, 3423–3434.

